Differential cross sections for secondary electron production by proton impact

M. E. Rudd
Department of Physics and Astronomy, University of Nebraska–Lincoln, Lincoln, Nebraska 68588-0111
(Received 17 March 1988)

The differential cross section for ionization of atoms and molecules by proton impact is modeled over a wide range of incident-proton and ejected-electron energies by an analytical equation. This equation is based on the molecular promotion model at low energies and on the classical binary-encounter approximation, modified to agree with the Bethe theory of ionization, at high energies. Three adjustable parameters are sufficient to fit the experimental electron energy distribution at any given impact energy. Equations are given which fit two of these parameters as a function of proton energy over the range of 5 keV to 5 MeV. The third parameter is found to be a constant, independent of proton energy, but its value varies somewhat from target to target. The relation of one of these parameters to the optical oscillator strength is discussed as is the extension of the model to multishell targets. As examples, the model is applied to fit data on molecular hydrogen, helium, and argon. Quantities such as the stopping cross section, the average ejection energy, and the fraction of electrons ejected with energies greater than a given value are easily calculated using this model.

I. INTRODUCTION

The process involving the greatest energy transfer during collisions of protons with atoms or molecules is the ejection of electrons. Such secondary electrons, if sufficiently energetic, can themselves cause further ionization. The details of this process are of obvious importance in all studies involving energy deposition by fast ions moving through matter. Radiation damage in biological tissues and in other materials, the production of auroras, and studies of solar and stellar processes are examples of areas in which this type of data is required.

Measurements of total electron production cross sections by proton impact have been made at many laboratories starting in 1949. These data have recently been compiled and evaluated by Rudd *et al.*[1] Comprehensive measurements of differential cross sections for this process, however, have been made only by a few groups starting in the early 1960s. These were measurements of the angular and energy distributions of electrons ejected during the collisions. Such doubly differential cross sections (DDCS's) can be integrated over angle to obtain the singly differential cross sections (SDCS's) which are the focus of the present work. While the general agreement between the various groups measuring DDCS's is fairly good, there are sizable discrepancies in some ranges of parameters. Low-energy electrons (below about 10 eV) are especially difficult to control and measure accurately and therefore large discrepancies appear among the data in that region. One purpose of the present study is to provide a basis for settling such disagreements and to provide recommended values for the SDCS for a variety of targets.

Attempts to calculate these cross sections theoretically date back at least to 1912. Besides the classical binary encounter approximation (BEA) (Refs. 2–7) and the Born approximation,[8–10] Monte Carlo methods[11–13] have also been employed to obtain differential cross sections. Although each of these methods has had some success, they are all limited to high projectile velocities, i.e., velocities greater than the orbital velocity of the electrons in the target atoms. The Born approximation also requires accurate knowledge of the initial and final-state wave functions, a requirement which is difficult to meet except for the simplest monatomic targets.

Miller and co-workers[14–16] have developed a semiempirical model for the SDCS based on the Bethe theory of energy loss. The soft-collision component of the cross section is calculated from photoionization data and the hard-collision component is obtained by subtracting the soft-collision part from the experimental data at one proton energy. This component is merged into the BEA cross sections at the highest electron energies. This model has proved useful for both electron and ion impact but it, too, is applicable only for fast projectiles.

Recently Inokuti *et al.*[17] introduced a model, based on the Bethe theory, for the secondary electron spectra from collisions of charged particles with atoms and molecules. In this model the Bethe parameter dependence on electron energy is fitted by polynomial expressions with twelve adjustable fitting parameters. This model applies only to high-energy collisions for which the ejected electron energy is not too great.

In the low-velocity region the most promising theoretical method is the molecular promotion model of Fano and Lichten.[18] The only application of this model to the calculation of SDCS's is that of Rudd[19] who with Macek derived an exponential dependence of the cross section on the secondary electron energy. However, this model did not yield absolute values of the SDCS and the relative values had discrepancies as large as a factor of 2.

In the present paper a simple analytical expression is developed which is based on the BEA, the Bethe approximation, and on the molecular promotion model. With three adjustable fitting parameters it is possible to fit the SDCS's for all electron energies at a single proton energy.

One of these three parameters is approximately independent of proton energy for a given target. A study of the variation of the other two parameters with proton energy allows a connection to be made to the generalized oscillator strength at high energy and with the parameters describing the total cross-section dependence on proton energy[1] at low energy. A report on a preliminary version of this model was presented earlier.[20]

In addition to the adjustable parameters, the model requires knowledge of the number of electrons in each subshell of the target atom and their binding energies. In the case of targets with more than one subshell, the partial cross sections for the various subshells are calculated separately and added.

The present model allows users to make rapid calculations of needed cross sections at any combination of projectile and secondary electron energy. Knowing the fitting parameters for a given target allows one to easily calculate not only SDCS's, but also, by integration, such quantities as the total electron ejection cross section, the stopping cross section due to ionization, the average ejected electron energy, and the fraction of electrons ejected with energies greater than the binding energy. Since the model provides a compact expression describing the systematics of secondary electron production, it may also prove helpful in developing new theoretical approaches to the calculation of cross sections.

In Sec. II the model is developed by combining previous collision models. Before fitting the model to the experimental data, the measured SDCS's were adjusted so that their integral agreed with accepted values of the total cross section. This adjustment is discussed in Sec. III. In Sec. IV the process of fitting the model to each energy spectrum is described and in Sec. V the fitting of the parameters as a function of proton energy is considered. Approximate equations for the integral of the SDCS's are given in Sec. VI where the relation of one of the parameters to the generalized oscillator strength is shown. Multishell targets are discussed in Sec. VII and a calculation of quantities derived from the cross sections are given in Sec. VIII. Section IX discusses the extension of this model for use with other projectiles.

II. DEVELOPMENT OF THE MODEL

A. Large primary energies

Consider first a one-electron atom with a binding energy R ($=13.6$ eV). The BEA equation for low ejected-electron energies may be written

$$\sigma(W)=4\pi a_0^2 R^2[f_1(T)+f_2(T)W]/(W+R)^3 , \quad (1)$$

where $f_1(T)=7R/3T$ and $f_2(T)=1/T$. W is the ejected electron energy, T is the proton energy E_p divided by λ, the ratio of the mass of the projectile to the electron mass, and a_0 is the radius of the first Bohr orbit. This equation, first given by Williams[3] in 1927, was an improvement on the earlier calculation of Thomson[2] in that it took account of the motion of the electron in the target. However, Williams incorrectly assumed that all ejection angles were available to the outgoing electron regardless of the energy transfer, a mistake that subsequent authors[4-7] corrected. In the present model this correction is made in a different way.

Bethe's treatment of the Born approximation[21] yields

$$\sigma(W)=4\pi a_0^2 R^2[g_1(W)\ln(4c_E T/R)/T+g_3(W)/T^2] ,$$

where $g_1(W)=(1/E)df/dE$, $E=W+R$, df/dE is the differential optical oscillator strength, and c_E is a function of W. The quantity $g_1(W)\ln(4c_E)$ can be renamed $g_2(W)$ yielding

$$\sigma(W)=4\pi a_0^2 R^2[g_1(W)\ln(T/R)/T+g_2(W)/T+g_3(W)/T^2] . \quad (2)$$

Equations (1) and (2) can both be satisfied by choosing somewhat different expressions for f_1 and f_2, namely,

$$f_1(T)=(A_1 R/T)\ln(T/R)$$

and (3)

$$f_2(T)=A_2/T+B_2 R/T^2 ,$$

where A_1, A_2, and B_2 are dimensionless constants, and by setting

$$g_1(W)=A_1 R/(W+R)^3 ,$$

$$g_2(W)=A_2 W/(W+R)^3 , \quad (4)$$

and

$$g_3=B_2 RW/(W+R)^3 .$$

Equation (1) can be generalized slightly to hold for the ionization of an atomic subshell with N electrons and a binding energy I. At the same time, we introduce the dimensionless quantities $w=W/I$, the reduced electron energy, and $v=(T/I)^{1/2}$, the reduced projectile velocity. Then Eq. (1) becomes

$$\sigma(w)=(S/I)(F_1+F_2 w)/(1+w)^3 , \quad (5)$$

where $S=4\pi a_0^2 N(R/I)^2$ and where F_1 and F_2 are functions of v which reduce to f_1/R and f_2 in the high-energy limit.

Equation (5) indicates that a plot of $(1+w)^3\sigma(w)$ versus w should be a straight line with a slope of F_2 and an intercept of Fig. 1. Figure 1 shows for the example of 500-keV $H^+ + H_2$ that this prediction is realized up to a cutoff energy $w_c=W_c/I$. Beyond that point the cross section follows a different dependence.

The origin of the cutoff energy can be understood on the basis of the BEA in which the proton is assumed to collide only with the electron. For such a collision, momentum and energy conservation dictate that above a certain ejection energy the range of possible recoil angles begins to be restricted causing a rapid drop in the cross section. BEA theory gives $W_c=4T-\gamma(IT)^{1/2}$ for this cutoff energy with $\gamma=4$. However, experimentally we find that $\gamma=2$ fits the data much more closely. In our notation, then, the cutoff is at $w_c=4v^2-2v$. As the impact energy decreases, the cutoff energy decreases and eventually the region above the cutoff encompasses the

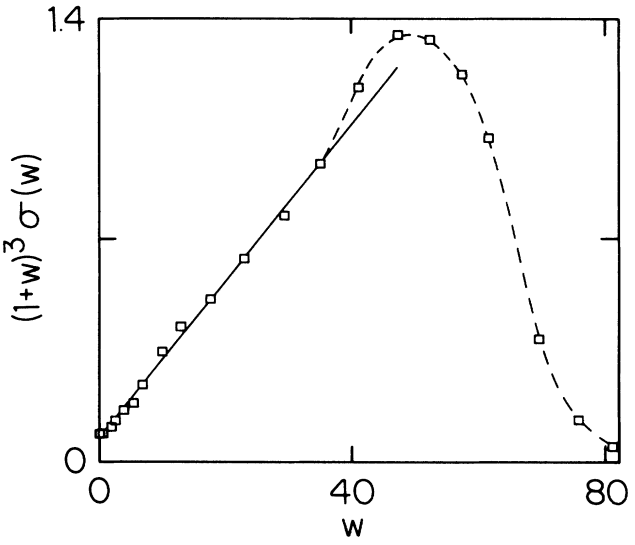

FIG. 1. Plots of cross section multiplied by $(1+w)^3$ to show linear dependence up to the cutoff energy. Data are for 500-keV proton collisions with H_2 (Ref. 22).

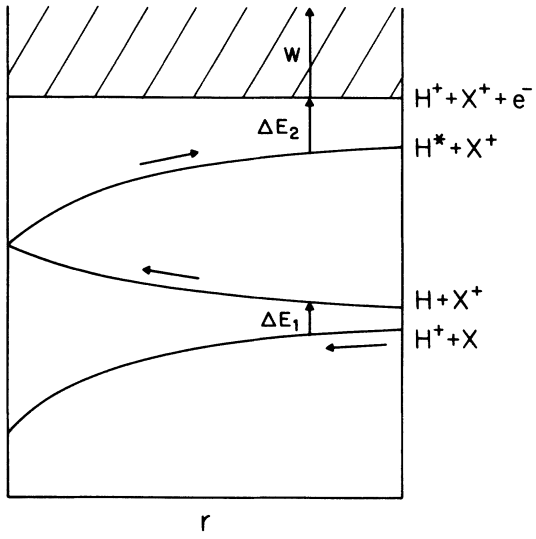

FIG. 2. Schematic correlation diagram showing the electron transfer transition, molecular promotion, and transition into the continuum. r is the internuclear separation.

entire energy range of ejected electrons.

Above the cutoff experiment yields a nearly exponential decrease in the cross section. The logarithmic slope in this region is found to vary with impact energy in a systematic way such that the cross section has an $\exp[-\alpha(w-w_c)/v]$ dependence where α is a dimensionless constant near unity. The value of α varies from 0.6 to 0.9, varying slightly from target to target. This factor can be combined with the expression in Eq. (5) by writing

$$\sigma(w)=(S/I)(F_1+F_2w)(1+w)^{-3} \times\{1+\exp[\alpha(w-w_c)/v]\}^{-1} . \quad (6)$$

For $w \ll w_c$ this reduces to Eq. (5). For $w \gg w_c$ the exponential factor dominates the cross section.

B. Small primary energies

Rudd[19] and Macek applied the molecular promotion model to obtain an equation for the SDCS at small impact energies. This was derived from Meyerhof's expression for transition probabilities[23] which was based on Demkov's treatment of charge transfer.[24]

Referring to the schematic correlation diagram in Fig. 2, during a collision there is first an electron capture transition, $H^+ + X \rightarrow H + X^+$ involving an energy difference ΔE_1 followed by a promotion through a rotational coupling to an excited state of H. A subsequent transition into the continuum takes place with an energy difference $\Delta E_2 + W$ where W is the kinetic energy of the ejected electron. The energy differences are given approximately by $\Delta E_1 = I - R$ and $\Delta E_2 = R/4$.

We define $w_1 = \Delta E_1/I \cong 1 - R/I$ and $w_2 = \Delta E_2/I \cong R/4I$ and also note that if $I < R$, the curves must cross and so $w_1 = 0$. Application of the Meyerhof equation to the two transitions yields the probabilities $P_1 = 1/(1+\exp 2x_1)$ and $P_2 = 1/(1+\exp 2x_2)$ where $x_1 = l\Delta E_1/2\hbar v_p$ and $x_2 = l(\Delta E_2 + W)/2\hbar v_p$ and where v_p is the proton velocity and l is a characteristic length approximately equal to the diameter of the atomic shell. We set $l = 2a_0\alpha(R/I)^{1/2}$ where α is a dimensionless length parameter near unity which will be identified with the α in Eq. (6). Also $v_p = v_0(T/R)^{1/2}$ where v_0 is the velocity associated with the first Bohr orbit. Then using the relation $2Ra_0 = \hbar v_0$ the probabilities may be written $P_1 = 1/(1+\exp\alpha w_1/v)$ and $P_2 = 1/[1+\exp\alpha(w+w_2)/v]$. The cross section for the entire process is then

$$\sigma(w) = \sigma_{RC}(v) P_1(v) P_2(w,v) , \quad (7)$$

where σ_{RC} is the rotational coupling cross section. The form of P_2 is very similar to that of the factor in Eq. (6) containing the exponential. They would be identical if $w_c \rightarrow -w_2$ at low energies and if $w_c \rightarrow 4v^2 - 2v$ at high energies. These conditions can both be satisfied simply by setting

$$w_c = 4v^2 - 2v - w_2 . \quad (8)$$

Then the factor which describes the high-energy behavior above the cutoff merges into the probability $P_2(w,v)$ at low impact energies. Since σ_{RC} is an unknown function of v, it is simply absorbed into the other factors of Eq. (6) along with $P_1(v)$. The final form of the model equation is then

$$\sigma(w)=(S/I)[F_1(v)+F_2(v)w](1+w)^{-3} \times\{1+\exp[\alpha(w-w_c)/v]\}^{-1} , \quad (9)$$

with w_c given by Eq. (8).

It is also possible that transitions into the continuum take place at or near the distance of closest approach. This would not change the results except to increase slightly the value of w_2.

III. ADJUSTMENT OF DATA

DDCS's have been measured for a variety of targets and proton energies. For helium and argon there are compilations in the literature.[25,26] These data sets have also been integrated over angle to yield the SDCS's differential in ejected electron energy which are of interest here. These, in turn, can be integrated over electron energy to yield the total electron ejection cross sections $\sigma_- = \int_0^\infty \sigma(W)dW$. This is a good check on the accuracy of the DDCS and SDCS data since recommended values of σ_- are available[1,27] for a large number of targets over wide energy ranges. The experimental SDCS's at each impact energy were adjusted so that the integral of each one matched the corresponding σ_- cross section given in Ref. 1 before Eq. (9) was fitted to it.

Two methods of adjustment were used, the first being a simple multiplication of all SDCS's in a data set by the same factor. However, in most data sets the cross sections for low ejected electron energies have a larger uncertainty than those for intermediate and high electron energies. For such data sets, a larger adjustment was made in the low-energy region. In this case, adjusted cross sections $\sigma(W)$ were calculated from the equation:

$$\sigma(W)/\sigma_u(W)=[1+K_c\sigma_u(W)/\sigma_u(0)]^{1/K_c}-1 ,$$

where $\sigma_u(W)$ is the unadjusted value and $\sigma_u(0)$ is the cross section at the lowest energy in the data set. K_c is chosen to make the integral equal to the tabulated total cross section. A judgment had to be made concerning which method of adjustment to use for a particular data set based on the relative uncertainties in the different energy ranges. Most of the data sets from the Pacific Northwest Laboratory,[22,25,26] for example, were taken using time-of-flight methods at low electron energy and therefore have a nearly constant accuracy over the entire energy range while data taken with electrostatic analyzers are usually less accurate at low energies. In either case, data below 2 eV were considered to have too large an uncertainty to use in the fitting.

IV. FITTING TO THE DATA

Equation (9) was fitted to a data set at a given proton energy using F_1, F_2, and α as adjustable fitting parameters. A nonlinear least-squares fitting routine was adapted from the CURFIT program of Bevington[28] which is based on Marquardt's method.[29] Data for molecular hydrogen from 20 runs at 16 different proton energies were fitted in this way taking $N=2$ and $I=15.4$ eV. At some of the higher impact energies the entire range of the data falls below the cutoff w_c making a determination of the values of α impossible for those energies. The average deviation for the fits was 9% while the uncertainty in the experimental data itself was 15–20%. Figure 3 shows typical fits for five of the proton energies. In this graph the dimensionless quantity $\log_{10}(I/S)(1+w)^2\sigma(w)$ was plotted versus $\log_{10}w/v$. The factor $(1+w)^2$ reduces the range of variation of the cross sections which, for some runs, was as great as six orders of magnitude. Figure 4 shows the variation of the three fitting parameters with proton energy.

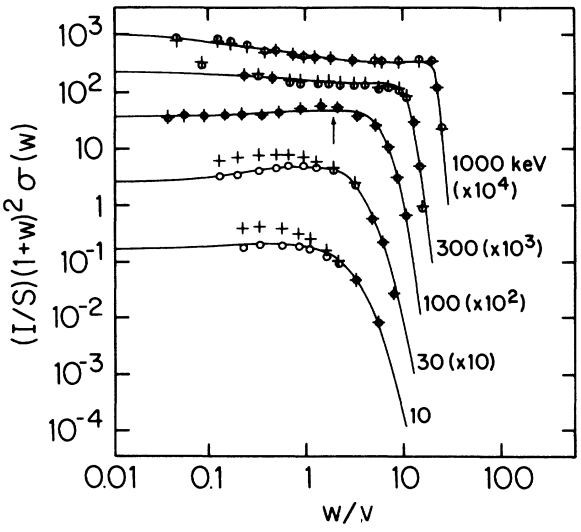

FIG. 3. Fit of the model to electron energy distributions for protons on molecular hydrogen. Cross sections are multiplied by $(I/S)(1+w)^2$. The crosses are the unadjusted and the circles the adjusted experimental data (Refs. 19, 22, and 30). The lines are the model calculations.

Helium data from 38 runs done at five different laboratories at energies from 5 to 5000 keV were also fitted using $N=2$ and $I=24.6$ eV yielding an average deviation of 11%. In Fig. 5 samples of the data for helium are shown along with the model calculations. For comparison the results of a calculation using the distorted-wave Born approximation (DWBA) (Ref. 10) are also plotted. While the DWBA describes the high-energy cross sections accurately, the discrepancy increases as the proton energy decreases.

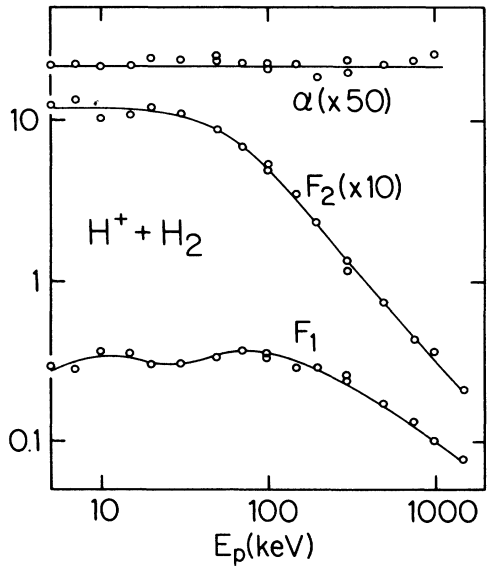

FIG. 4. Variation of the three fitting parameters with proton energy for hydrogen.

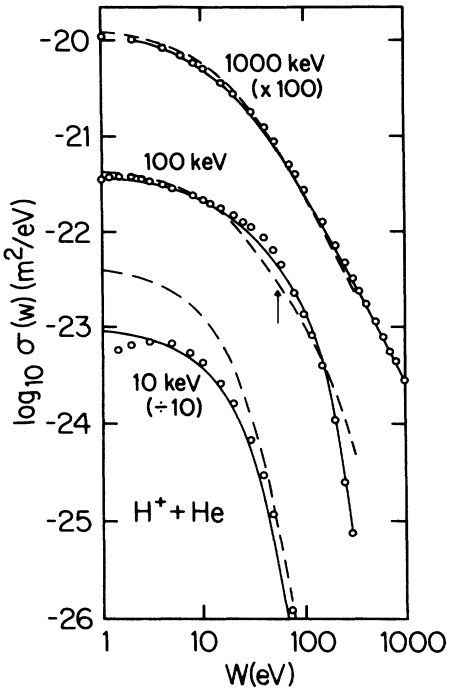

FIG. 5. Energy spectra of electrons from proton-helium collisions. Circles are the adjusted experimental data (Ref. 25); dashed lines are calculated cross sections using the distorted-wave Born approximation. Solid lines are the model calculations with F_1 and F_2 calculated from Eq. (10). The arrow shows the expected position of the peak due to electron transfer to the continuum.

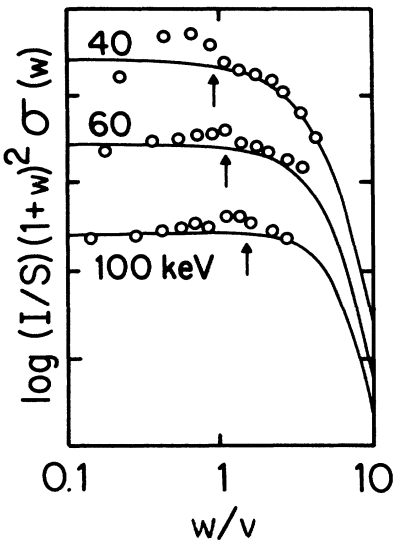

FIG. 6. Fit of the model to differential cross section data for protons on hydrogen. The circles are the adjusted data of Gibson and Reid (Ref. 31). The line is the model calculation using parameters from Eq. (10). The vertical arrows indicate the expected positions of the electron transfer to the continuum peak.

The model does not include Auger or autoionization electrons nor any contribution due to the mechanism of electron capture to the continuum. This latter mechanism causes a small additional peak in the cross-section curve at an electron velocity equal to the proton velocity; a peak which is noticeable in the 100-keV curves in Figs. 3 and 5, for example. The vertical arrows indicate the expected positions of the peaks. Since the effect of this mechanism is most pronounced at small angles, the peak is more prominent in the data of Gibson and Reid,[31] Fig. 6, whose data extends to 0°. In the other data sets the smallest angle measured was 10° or 15°. The tendency of the peaks to be centered at slightly lower than expected energies may be due in part to the range of angles included.

V. FITTING $F_1(v)$ AND $F_2(v)$

As seen in Fig. 4, the parameter α varies only slightly over the entire range of impact energies and was taken to be a constant for any one target. The fitting parameters F_1 and F_2, however, vary with impact energy so those parameters themselves should be describable by functions of v. They were fitted by the equations

$$F_1 = L_1 + H_1 \text{ and } F_2 = L_2 H_2/(L_2+H_2) ,$$

where

$$H_1 = A_1 \ln(1+v^2)/(v^2+B_1/v^2) ,$$
$$H_2 = A_2/v^2 + B_2/v^4 , \tag{10}$$
$$L_1 = C_1 v^{D_1}/(1+E_1 v^{(D_1+4)}) \text{ and } L_2 = C_2 v^{D_2} .$$

In the high-energy limit these expressions reduce to f_1/R and to f_2 in Eq. (3). $A_1, \ldots, E_1$ and $A_2, \ldots, D_2$ plus α are the ten basic fitting parameters for each target. Some of these parameters can be related to better-known quantities as will be shown. The fits to these equations for hydrogen are shown in Fig. 4. The values of the basic parameters for three target gases are given in Table I. If instead of adjusting F_1, F_2, and α for the best fit for each experimental data set, we take α to be the average of the

TABLE I. Values of the basic parameters.

	Hydrogen	Helium	Argon	Inner shells[a]
A_1	0.80	1.00	1.10	1.25
B_1	2.9	3.3	1.50	0.5
C_1	0.86	1.31	1.84	2.0
D_1	1.48	2.1	0.78	2.0
E_1	7.0	1.92	8.1	3.0
A_2	1.06	0.84	1.20	1.1
B_2	4.2	5.0	0.10	1.3
C_2	1.39	0.84	1.15	1.0
D_2	0.48	1.04	0.74	0.3
α	0.87	0.86	0.72	0.62
A_1[b]	0.80	0.89	1.20	

[a]Approximate values.
[b]Value of A_1 from Eq. (15).

fitted values and calculate F_1 and F_2 from Eq. (10), the deviations from experiment are somewhat greater but still generally within the experimental uncertainty.

VI. INTEGRATION OF THE MODEL EQUATION

The SDCS given by Eq. (9) may be integrated numerically over the ejected electron energy to obtain the total electron ejection cross sections σ_-. It may be integrated analytically by making approximations. One way to do this is to set

$$\sigma_- = S\int_0^{w_c}(F_1+F_2 w)(1+w)^{-3}dw + S\int_{w_c}^{\infty}(F_1+F_2^{w})(1+J^{-1}\exp\alpha' w/v)^{-1}dw \quad \text{if } w_c \geq 0 , \tag{11}$$

and

$$\sigma_- = S\int_0^{\infty}(F_1+F_2 w)(1+J^{-1}\exp\alpha' w/v)^{-1}dw \quad \text{if } w_c \leq 0 ,$$

where $\alpha' = \alpha + 3v$ and $J = \exp(\alpha w_c/v)$. The second part of the second integral cannot be done exactly, but an approximation based on the first term of an expansion will suffice for this purpose. The result is

$$\sigma_- = S\{w_c(1+w_c)^{-2}[w_c(F_1+F_2)/2+F_1] + (v/\alpha')[F_1+F_2(v/\alpha'-w_c)] \times \ln(1+J\exp-\alpha' w_c/v)\} \quad \text{for } w_c \geq 0 \tag{12}$$

and

$$\sigma_- = S(v/\alpha')(F_1+F_2 v/\alpha')\ln(1+J) \quad \text{for } w_c \leq 0 .$$

This expression gives a total cross section which agrees very well with that obtained by numerical integration at high energies and reasonably well at low energies. In the intermediate energy region there are discrepancies on the order of 25%.

A. High-energy asymptotic expression

At large proton energies, a considerable simplification in Eq. (12) results. From Eqs. (8) and (10), $F_1 = A_1\ln(v^2)/v^2$, $F_2 = A_2/v^2$, and $w_c = 4v^2$ when $v \gg 1$, so Eq. (12) reduces to

$$\sigma_- = (S/2v^2)[A_1\ln(v^2)+A_2] .$$

To compare with the Bethe equation this may be rewritten in different notation:

$$\sigma_- = (2\pi a_0^2 NR^2/IT)[A_1\ln(T/R)+A_1\ln(R/I)+A_2] . \tag{13}$$

The high-energy limit of the fitting equation used for the total cross sections by Rudd *et al.*[1] was

$$\sigma_- = (4\pi a_0^2 R/T)[A\ln(T/R)+B] , \tag{14}$$

where A and B are two of the four fitting parameters used in that compilation. This equation is equivalent to the Bethe equation and the quantity A is identical to the generalized oscillator strength obtained from photoionization experiments as shown in Ref. 1. A comparison of Eqs. (13) and (14) yields

$$A_1 = 2AI/NR . \tag{15}$$

The comparison could also provide an expression for A_2 but the quantities B from Ref. 1 and A_2 in this model are both affected by the rest of the equation in different ways and therefore are not comparable. A different relation for A_2 will be derived in Sec. VIII.

B. Low-energy asymptotic expression

For $v \ll 1$, $w_c = -w_2$, $F_1 = C_1 v^{D_1}$, $F_2 = C_2 v^{D_2}$, and $\alpha' = \alpha$. Then, Eq. (12) reduces to

$$\sigma_- = 4\pi a_0^2\alpha^{-1}N(R/I)^2(C_1 v^{(D_1+1)}+C_2 v^{(D_2+1)}) \times \exp(-\alpha w_2/v) .$$

Since w_2 is small, the exponential factor does not differ much from unity except at very low projectile energies. If that factor is neglected, this expression can be compared to the low-energy expression for the total cross section given in Ref. 1 which is $\sigma_- = 4\pi a_0^2 C(T/R)^D$ where C and D are tabulated for various targets. This comparison is not sufficient to determine values of C_1, C_2, D_1, and D_2, but an important condition can be obtained, namely, that $D_1 \geq 2D-1$ and $D_2 \geq 2D-2$. In fitting the parameters F_1 and F_2, the data often do not extend to a low enough energy to determine D_1 and D_2 accurately and so in some cases the fits have been adjusted to conform to these conditions using the values of D from Ref. 1.

VII. MULTISHELL TARGETS

Targets with more than one shell can be treated by calculating the partial cross section for each subshell characterized by its own N_i and I_i, and adding the contributions to obtain the SDCS. Then Eq. (9) becomes

$$\sigma(w) = \sum_i (S_i/I_i)(F_{1i}+F_{2i}w_i)(1+w_i)^{-3} \times \{1+\exp[\alpha_i(w_i-w_{ci})/v_i]\}^{-1} . \tag{16}$$

The other equations are modified in an obvious way by summing over i and subscripting the variables I, v, w, w_c, F_1, F_2, and α. In Eq. (5) NR/I is replaced by $\sum_i N_i R/I_i$.

Unfortunately, experimental data on ejection of electrons from individual shells of multishell atoms or molecules are very limited. Some σ_- data exist, but no SDCS's have been measured. Sarkadi *et al.*[32] have measured angular distributions of electrons from the L shell of argon but only at three electron energies and one proton energy. In the absence of such data there is no direct way to determine the values of the basic parameters $A_1, \ldots, D_2$ and α for the separate shells. However, some progress can be made in a less direct way.

Electrons from the the outermost subshell are the least tightly bound and usually dominate the SDCS except at

the higher electron energies where inner-shell electrons become relatively more important. We divide the inner subshells of a given atom or molecule into two categories; (a) those subshells which are not much different in binding energy from the outermost shell and (b) deeper inner shells. The boundary between these two categories was arbitrarily taken to be at a binding energy equal to two times the outermost subshell binding energy. The less tightly bound inner shells probably do not differ greatly in the values of the basic parameters from the outermost subshell, so as an approximation the same values of those parameters are used. Most of the subshells of molecular targets fall into this category as well as the outer s shells of the rare gases.

On the other hand, the deeper inner shells are relatively independent of the outer-shell configurations and are similar from target to target. Garcia[33] has shown, e.g., using x-ray data, that the total cross sections for K- and L-shell ionization of heavy atom targets by protons follow a universal curve when $I^2\sigma_-$ is plotted versus $E/\lambda I$ (which is v^2 in the notation of this paper). Stolterfoht and Schneider[34] and others have also shown this from Auger electron data for gases. Basbas *et al.*[35] starting from the plane-wave Born approximation, arrived at essentially the same universal curve but went on to improve the scaling by adding corrections for the change in effective binding energy at low energies and for nuclear Coulomb deflection of the projectile path. For the present purposes, we will not take these latter refinements into account.

The present model also predicts a universal curve for the deep inner shells with large binding energies. Since $I \gg R$ for such shells, $w_2=0$ and $w_c=4v^2-2v$. So for deep inner shells w_c is a function only of v and depends on the binding energy I only through v. Then from Eq. (12) we can see that the cross section σ_- multiplied by I^2/N is a function only of v provided that F_1, F_2, and the constant α are independent of the target. As seen in Fig. 7, F_1 and F_2 are nearly independent of the target for high velocities although there are some variations at low velocities. For deep inner shells the variations are likely to be even smaller. Thus the present model also predicts a universal curve for ejection of electrons from deep inner shells.

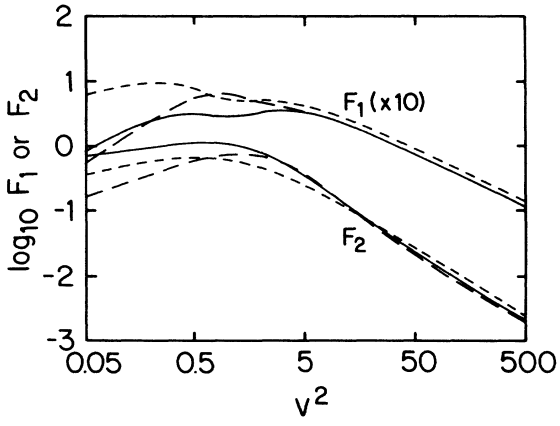

FIG. 7. Values of the parameters F_1 and F_2 vs the reduced projectile velocity squared for hydrogen (solid line), helium (long-dashed line), and argon (short-dashed line).

TABLE II. Values of N and I for argon.

Subshell	N	I (eV)
$3p$	6	15.8
$3s$	2	29.2
$2s+2p$	8	263

Estimated values of some of the basic parameters for inner shells were obtained from the SDCS data on argon[26] where, at some proton energies, cross sections were measured at a high enough electron energy that the contribution from the $n=2$ shell dominates. Unfortunately, fitting the model in this restricted region was not sufficient to determine all ten parameters, but estimates of the others could be made by choosing them so as to agree with the universal curve of total inner-shell cross sections. The rough approximate values of the inner-shell basic parameters obtained this way are given in Table I. If SDCS data for ejection of inner shell electrons become available in the future, these parameters can be determined with greater accuracy.

Using these inner-shell parameters, calculations have been made for argon. The values of N_i and I_i used are

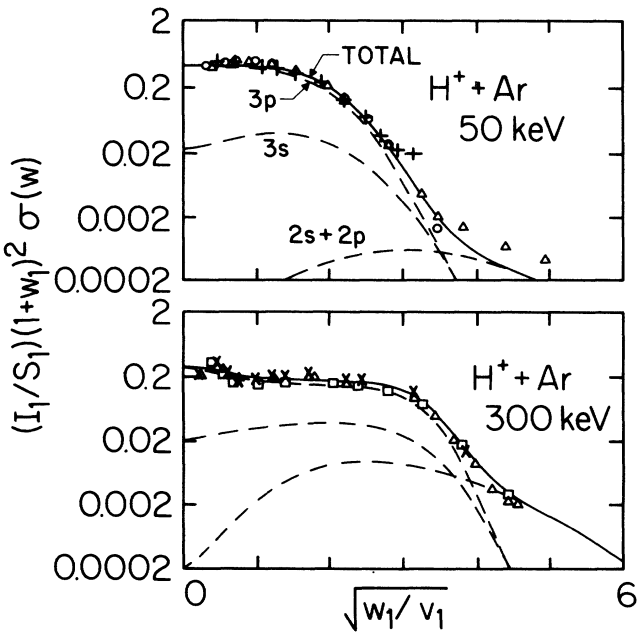

FIG. 8. Fit of the model to differential cross section data for protons on argon. Contributions from the $3p$, $3s$, and the $2p+2s$ subshells are shown along with the total. Circles, data of Rudd (Ref. 26); triangles, data of Crooks and Rudd (Ref. 26); crosses, data of Criswell and Toburen (Ref. 26, 50 keV) and of Toburen (Ref. 26, 300 keV); squares, data of Gabler *et al.* (Ref. 26).

given in Table II. A weighted average of the values of I for the $2p$ and $2s$ subshells was used. The results are given in Fig. 8 for two proton energies which show the contributions from these subshells along with the total compared to the experimental values. For argon, the $3p$ shell contribution is dominant at the lower electron energies, and the $3s$ shell makes only a minor contribution since it contains only two electrons, but, as noted above, the relative contribution from the $2p$ and $2s$ subshells increases at higher energies, eventually becoming dominant. While the $2s+2p$ contribution is underestimated at 50 keV, the agreement is quite good at 300 keV.

VIII. APPLICATIONS

The availability of a model of the SDCS such as the present one enables one to make calculations of a number of quantities which are of interest in a variety of applications. The average ejected electron energy W_{av}, the stopping cross section due to ionization σ_{st}, and the fraction f_I of ejected electrons with sufficient energy to cause further ionization are defined in terms of the SDCS:

$$\sigma_{st}=(1/R)\int_0^\infty (W+I)\sigma(W)dW \ , \tag{17}$$

$$W_{av}=(1/\sigma_-)\int_0^\infty W\sigma(W)dW \ , \tag{18}$$

and

$$f_I=(1/\sigma_-)\int_I^\infty \sigma(W)dW \ . \tag{19}$$

Values for these quantities may be obtained from numerical integration of the cross sections or by approximation equations derived in a manner similar to that used for Eq. (11). For the stopping cross section the result of such an approximation is

$$\sigma_{st}=(SI/R)[(F_1-F_2)w_c(1+w_c)^{-1}+F_2\ln(1+w_c) +(v/\alpha'')(F_1+F_2v/\alpha'')\ln(1+\exp-2w_c)] \quad \text{for } w_c\geq 0 \tag{20}$$

and

$$\sigma_{st}=(SI/R)(v/\alpha'')(F_1+F_2v/\alpha'')\ln(1+J) \quad \text{for } w_c\leq 0 \ ,$$

where

$$J=\exp(\alpha w_c/v) \text{ and } \alpha''=\alpha+2v \ .$$

For $v\gg 1$ this reduces to

$$\sigma_{st}=4\pi a_0^2(RN/T)(A_1+A_2)\ln(T/R) \ ,$$

where $N=\sum_i N_i$. This may be compared to the Bethe result[21]

$$\sigma_{st}=8\pi a_0^2(RN/T)\ln(T/R) \ ,$$

yielding the important condition on the basic parameters $A_1+A_2=2$. In Table I it may be seen for the three targets studied that this condition is approximately satisfied. Alternatively, A_2 could be obtained from this equation after A_1 is found from the generalized oscillator strength using Eq. (15).

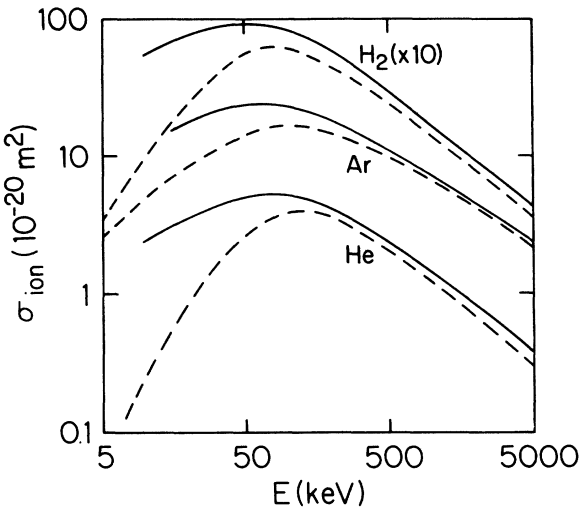

FIG. 9. Stopping cross sections for three targets. Dashed lines, stopping cross section contributed by ionization as calculated from the model; solid lines, total stopping cross sections (Ref. 36).

Values of the stopping cross sections for the three targets calculated from Eq. (17) are shown in Fig. 9 along with measured values.[36] Ionization is expected to contribute 78–85 % of the total stopping cross section for hydrogen above about 300 keV.[37] As seen in the figure, the present model yields values of σ_{st} at high energies which are 83% of the total for H_2, 81% for He, and 87% for Ar, in very good agreement with expectations.

The average energy calculated from Eq. (18) for the three targets is shown in Fig. 10. This quantity increases with impact energy until the reduced velocity v is approximately unity. For hydrogen and helium it is nearly constant at higher energies but is still rising for argon at 5

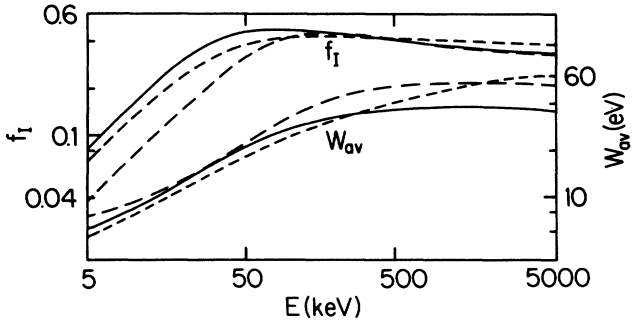

FIG. 10. Top: calculations from the model of the fraction of electrons ejected with energies greater than the first ionization potential; scale on the left. Bottom: average ejection energies for three targets calculated from the model; scale on the right. Solid lines, hydrogen; long-dashed lines, helium; short-dashed lines, argon.

MeV because of the influence of inner shells.

An unexpected feature of the curves of f_I, calculated from Eq. (19) and shown in Fig. 10, is that the fraction of electrons ejected with an energy above the first ionization potential actually decreases with impact energy above $v=1$.

IX. EXTENSIONS OF THE MODEL

The model is also applicable to impact by any other bare nucleus. If Z^2 scaling is applicable, the calculation is particularly simple. Such scaling has been found by Toburen and Wilson[38] to hold for 300–2000-keV $He^{2+}+Ar$ collisions over most of the range of parameters studied. A discrepancy at small angles and at ejected electron velocities close to the projectile velocity is due to electron transfer to the continuum. Their SDCS data are fitted quite well by the present model without further adjustment except for the discrepancy at the equal velocity point already noted. The model is not appropriate for collisions by projectiles carrying electrons since there is no provision in it for electrons ejected from the projectile.

It appears from preliminary work that this model can also be applied to electron impact. In that case, of course, there is no promotion mechanism so the factor involving the exponential is not present. Additional effort in this direction is underway.

X. CONCLUSIONS

A model has been developed which describes the cross section for production of electrons by proton impact on atoms or molecules over a wide range of proton and ejected electron energies. It is based on the promotion model at low impact energies but merges continuously into an expression at high energies which is consistent with the Bethe theory. In multishell atoms and molecules the contribution from each subshell is computed from the values of N, the number of electrons and I, the binding energy for that subshell. The average deviations of the model from experimental values are generally within the experimental uncertainty of the measurements. Integration of the SDCS calculations in various ways by numerical methods or by approximations yield average ejected electron energies, stopping cross sections due to ionization, and fractions of electrons ejected in a given energy range.

ACKNOWLEDGMENTS

The author wishes to thank L. H. Toburen, N. Stolterfoht, and D. K. Gibson for supplying tables of experimental cross sections that were used in this study and D. H. Madison for providing the Born approximation calculations. He also wishes to thank Y.-K. Kim, J. Macek, and M. Inokuti for making helpful comments on the manuscript. This paper is based on work supported by the National Science Foundation under Grant Nos. PHY-8401328 and PHY-870105.

[1]M. E. Rudd, Y.-K. Kim, D. H. Madison, and J. W. Gallagher, Rev. Mod. Phys. **57**, 965 (1985).
[2]J. J. Thomson, Philos. Mag. **23**, 449 (1912).
[3]E. J. Williams, Nature **119**, 489 (1927).
[4]L. H. Thomas, Proc. Cambridge Philos. Soc. **23**, 713 (1927).
[5]Michal Gryzinski, Phys. Rev. **115**, 374 (1959); **138**, A322 (1965).
[6]E. Gerjuoy, Phys. Rev. **148**, 54 (1966).
[7]L. Vriens, Proc. Phys. Soc. **90**, 935 (1967).
[8]C. E. Kuyatt and T. Jorgensen, Jr., Phys. Rev. **130**, 1444 (1963).
[9]D. H. Madison, Phys. Rev. A **8**, 2449 (1973).
[10]M. E. Rudd and D. H. Madison, Phys. Rev. A **14**, 128 (1976).
[11]T. F. M. Bonsen and D. Banks, J. Phys. B **4**, 706 (1971).
[12]R. E. Olson and A. Salop, Phys. Rev. A **16**, 531 (1977).
[13]M. L. McKenzie and R. E. Olson, Phys. Rev. A **35**, 2863 (1987).
[14]J. H. Miller, L. H. Toburen, and Steven T. Manson, Phys. Rev. A **27**, 1337 (1983).
[15]W. E. Wilson, J. H. Miller, L. H. Toburen, and Steven T. Manson, J. Chem. Phys. **80**, 5631 (1984).
[16]J. H. Miller, W. E. Wilson, S. T. Manson, and M. E. Rudd, J. Chem. Phys. **86**, 157 (1987).
[17]Mitio Inokuti, Michael A. Dillon, John H. Miller, and Kazem Omidvar, J. Chem. Phys. **87**, 6967 (1987).
[18]U. Fano and W. Lichten, Phys. Rev. Lett. **14**, 627 (1965).
[19]M. E. Rudd, Phys. Rev. A **20**, 787 (1979).
[20]M. E. Rudd, Rad. Res. **109**, 1 (1987).
[21]H. Bethe, Ann. Phys. (Leipzig) **5**, 325 (1930); see also Mitio Inokuti, Rev. Mod. Phys. **43**, 297 (1971).
[22]L. H. Toburen and W. E. Wilson, Phys. Rev. A **5**, 247 (1972).
[23]W. E. Meyerhof, Phys. Rev. Lett. **31**, 1341 (1973).
[24]Yu. N. Demkov, Zh. Eksp. Teor. Fiz. **45**, 195 (1963) [Sov. Phys.—JETP **18**, 138 (1964)].
[25]M. E. Rudd, L. H. Toburen, and N. Stolterfoht, At. Data Nucl. Data Tables **18**, 413 (1976).
[26]M. E. Rudd, L. H. Toburen, and N. Stolterfoht, At. Data Nucl. Data Tables **23**, 405 (1979).
[27]M. E. Rudd, T. V. Goffe, R. D. DuBois, and L. H. Toburen, Phys. Rev. A **31**, 492 (1985).
[28]Philip R. Bevington, *Data Reduction and Error Analysis for the Physical Sciences* (McGraw-Hill, New York, 1969).
[29]Donald W. Marquardt, J. Soc. Ind. Appl. Math. **11**, 431 (1963).
[30]M. Eugene Rudd and Theodore Jorgensen, Jr., Phys. Rev. **131**, 666 (1963).
[31]D. K. Gibson and I. D. Reid, J. Phys. B **19**, 3265 (1986).
[32]L. Sarkadi, J. Bossler, R. Hippler, and H. O. Lutz, J. Phys. B **16**, 71 (1983).
[33]J. D. Garcia, Phys. Rev. A **1**, 1402 (1970).
[34]N. Stolterfoht and D. Schneider, Phys. Rev. A **11**, 721 (1975).
[35]George Basbas, Werner Brandt, and Roman Laubert, Phys. Rev. A **7**, 983 (1973).
[36]W. Whaling, in *Handbuch der Physik,* edited by S. Flugge (Springer-Verlag, Berlin, 1958), Vol. 34, pp. 173–217.
[37]W. E. Wilson, Radiat. Res. **49**, 36 (1972).
[38]L. H. Toburen and W. E. Wilson, Phys. Rev. A **1**, 2214 (1979).